Characterization and bond strength of electrolytic HA/TiO_2 double layers for orthopedic applications

CHI-MIN LIN, SHIOW-KANG YEN*
Department of Materials Engineering, National Chung Hsing University, Taichung, Taiwan 40227, ROC
E-mail: skyen@dragon.nchu.edu.tw

Insufficient bonding of juxtaposed bone to an orthopedic/dental implant could be caused by material surface properties that do not support new bone growth. For this reason, fabrication of biomaterials surface properties, which support osteointegration, should be one of the key objectives in the design of the next generation of orthopedic/dental implants. Titanium and titanium alloy have been widely used in several bioimplant applications, but when implanted into the human body, these still contain some disadvantages, such as poor osteointegration (forming a fibrous capsule), wear debris and metal ion release, which often lead to clinical failure. Electrolytic hydroxyapatite/titanium dioxide (HA/TiO_2) double layers were successfully deposited on titanium substrates in $TiCl_4$ solution and subsequently in the mixed solution of $Ca(NO_3)_2$ and $NH_4H_2PO_4$, respectively. After annealing at 300 °C for 1 h in the air, the coated specimens were evaluated by dynamic cyclic polarization tests, immersion tests, tensile tests, surface morphology observations, XRD analyses and cells culture. The adhesion strength of the HA coating were improved by the intermediate coating of TiO_2 from 11.3 to 46.7 MPa. From cell culture and immersion test results, the HA/TiO_2 coated specimens promoted not only cells differentiation, but also appeared more bioactive while maintaining non-toxicity.
© *2004 Kluwer Academic Publishers*

1. Introduction

Biomaterials must simultaneously possess many requirements and special properties such as non-toxicity, corrosion resistance, fatigue durability, and biocompatibility [1]. Titanium and titanium alloy biomaterials for implants have been widely applied to the orthopedic and dental fields [2]. These materials possess excellent corrosion resistance, good mechanical properties and biocompatibility. However, when titanium or titanium alloy is implanted into a complicated and aggressive physiological *in vivo* environment, the oxide stability may be affected, resulting in increasing metal ion release [3]. Titanium ions (in concentration ranging from 0.01 to 100 ng/ml) do not cause damage (in terms of cell viability or cell injury), but could inhibit phytohemagglutinin-induced T-cell or liposaccfaride-induced B-cell proliferation [4], and influence mineral formation [3]. In addition, titanium exhibits poor osteointegration properties [5] that also caused its incomplete fixation to living bone [6], and formation of fibrous capsule at the interface with the living bone [7]. Such fibrous capsule formation is a biological response to an implant and is important in the prevention of implant failure because the capsule isolates the foreign bodies in the biological environment and minimizes their adverse effects. Hydroxyapatite ($Ca_{10}(PO_4)_6(OH)_2$, HA) has excellent biocompatibility, promotes faster bone regeneration, and promotes direct bonding to regenerated bone without intermediate connective tissue [8]. However, the weak adhesion between HA and metal substrates is still the major problem [9–11]. Several methods have been suggested to improve the adhesion, such as co-sputtering of HA/Ti by RF magnetron [12], HA coating on Ti by ion beam dynamic mixing [13], pulse laser deposition [14], electrophoretic deposition and annealing [5, 15], sol-gel coating [16, 17], and hot isostatic pressing [18]. Therefore, we proposed a new concept using electrolytic deposition technology to prepare hydroxyapatite/titanium dioxide (HA/TiO_2) double layers on a Ti substrate. TiO_2 at the substrate surface not only acts as a chemical barrier against the release of metal ions from the implant, but also provides a chemical bonding between the titanium substrate and the HA coating to increase the adhesion strength. Porous bioactive HA coatings at the implant/body interface can enhance osteointegration. This HA/TiO_2 double layers on titanium implant surface should possess a good combination of biochemical stability and mechanical properties (particularly enhanced adhesion strength). The biocompatibility of HA/TiO_2 double layers was investigated by human G-292 osteoblast-like cells. Human G-292 osteoblast-like cells were found to be a valid experimental model for

*Author to whom correspondence should be addressed.

primary human osteoblast, expressing osteoblast mRNAs encoding osteocalcin, bone sialoprotein, alkaline phosphatase, α 1-collagen, epidermal growth-factor receptor, and BMP type II receptor [19]. Therefore, via observed cell adhesion and spreading morphology on surface-modified Ti implant, cell proliferation and differentiation were investigated. The surface morphology, phase transformation, bonding strength, electrochemical behavior, and biocompatibility were also characterized by scanning electron microscopy (SEM) and X-ray diffraction (XRD).

2. Experimental

2.1. Sample preparation

An ASTM F67 Grade 1 Ti sheet, as received, was used as a substrate of the deposition of the electrolytic calcium phosphate (CaP) coated and HA/TiO_2 double layers. It was cut into sheet thickness 0.8 mm. The sheet was then cut into discs with a diameter of 15 mm for dynamic cyclic polarization tests, tensile tests and immersion tests. All specimens were polished to a mirror finish with 1 μm Al_2O_3 powder, degreased with detergent and further ultrasonically cleaned in deionized water and acetone, and finally dried with N_2 gas gun.

2.2. Electrolytic deposition and annealing

The electrolytic deposition of HA/TiO_2 double layers were carried out in a 0.1-M $TiCl_4$ ethanol solution at pH = 1.52, $T = 25\,^{\circ}C$, and a cathodic current density of $1.0\,mA/cm^2$ for 300 s. Subsequently, the CaP and $TiO(OH)_2 \cdot H_2O$ coated specimens not allowed to dry were further deposited in a mixed solution of 0.042 M $Ca(NO_3)_2 \cdot 4H_2O$ and 0.025 M $NH_4H_2PO_4$ with Ca/P = 1.67, and at pH = 4.5, $T = 65\,^{\circ}C$, and a cathodic current density of $1\,mA/cm^2$ for 3000 s by using an EG&G M273A Potentiostat and M352 software. The titanium disc was the cathode, platinum the anode, and saturated AgCl/Ag the reference electrode. Both CaP and HA/TiO_2 coated specimens were then naturally dried and annealed for 1 h in the air at 300, 500, and 700 °C.

2.3. Dynamic cyclic polarization and immersion tests

To investigate corrosion resistance, the untreated, TGO-300 °C (thermally grown oxide annealed at 300 °C), EDT-300 °C (electrolytic deposition TiO_2 annealed at 300 °C), EDT-500 °C, EDT-700 °C, CaP-300 °C and HA/TiO_2-300 °C specimens were potentiodynamically polarized in aerated SBF solution of which composition is given as: Na^+ 142.0, K^+ 5.0, Ca^{+2} 2.5, Mg^{+2} 1.5, Cl^- 147.8, HCO_3^- 4.2, HPO_4^{-2} 1.0, and SO_4^{-2} 0.5 mM [22]. Analyzis was performed using EG&G Model 273A Potentiostat and M352 software. The cyclic polarization test ranged from −0.80 to +0.80 V, then back to −0.70 V at a scanning rate of 0.167 mV/s at 36 ± 1 °C. The first oxidation-reduction equilibrium potential E_{01} was derived when current density equaled zero while the applied voltage was increasing (forward cycle). If the oxidation was due to the corrosion of the electrode, this potential was also named ''corrosion potential'' E_{corr}. The current density before pitting was nearly constant and defined as the ''passivation current density'' i_{pass} [23]. Polarization resistance (R_p), defined as the slope of the potential-current density curve at the free corrosion potential, $R_p = (\Delta E/\Delta i)_{\Delta E \to 0}$. The polarization resistance was obtained for each specimen using the computer software (M352 software). Some untreated CaP-300 °C and HA/TiO_2-300 °C specimens were further immersed in aerated SBF solution at 36 ± 1 °C for one, three, seven, 14, and 21 days, because this annealing condition was the best one in the polarization tests. During the immersion test, the SBF solution does not change and after immersion for various periods, the specimens were gently washed with distilled water and dried in an oven at 50 °C. The apatite deposition or bioactivity during immersion was measured by determining the weight variation per unit area.

2.4. Tensile tests and cross-section observations

The bonding strength of CaP-300 °C (annealed at 300 °C) and HA/TiO_2-300 °C (annealed at 300 °C) layers to the substrate were measured by ASTM C-633 methods [20], because this annealing condition was the best one in the polarization tests. Both sides of the substrate (one side coated with CaP or HA/TiO_2) were attached to cylindrical steel clamps 15 mm in diameter and 20 mm in length by using Rapid-type Araldite glue [21]. Tensile load was normally applied to the substrates with a tensile testing system (MTS 810, USA) at a pull speed of 1 mm/min until fracture occurred. Both CaP-300 °C and HA/TiO_2-300 °C specimens were prepared in triplicate, with the mean bonding strength calculated from the fracture load and surface area $(\pi \times 7.5^2\,mm^2)$. The fractured surfaces of the specimens and the clamps were observed under a scanning electron microscope (SEM/EDS, JEOL JSM-5400, Japan).

The cross-section observations of the EDT-300 °C, CaP-300 °C and HA/TiO_2-300 °C samples were embedded in epoxy-resin. All samples cross-section were cut by a diamond blade to expose a fresh surface, and that fresh surface is then polished with the 1 μm Al_2O_3 power. Each sample was then coated with a thin layer of gold. The film thickness was examined by using a scanning electron microscopy and the composition energy determined by dispersive spectroscopy (SEM/EDS, JEOL JSM-5400, Japan).

2.5. SEM and XRD

The surface morphology of specimens after electrolytic deposition, tensile tests and immersion tests was observed by scanning electron microscopy and the composition energy determined by dispersive spectroscopy (SEM/EDS, JEOL JSM-5400, Japan). The crystal structure of CaP and HA/TiO_2 coatings on Ti substrate was analyzed by X-ray diffractomery (XRD) in a MAC MO3X-HF Diffractometer with CuK_α radiation (1.5418 Å), tube voltage 40 kV and current 30 mA. The angular range for 2θ was from 10° to 70° with a scanning rate of 2°/min.

2.6. Cell culture

Human osteoblast-like cell line G-292 (ATCC CRL 1423) [24] was originally isolated from a human osteosarcoma. Cells were initially cultured in McCoy's 5a medium containing 10% fetal bovine serum (FBS), 100 units/ml of penicillin and 100 μg/ml of strepotmycin. The cells were then thawed and cultured in 25 cm^2 flasks and incubated at 37 °C in a humidified atmosphere with 5% CO_2. Media were changed every two days. At confluence, cells were detached by trypsin treatment. After centrifugation, cells were resuspended in McCoy's 5a medium containing 10% FBS. Finally, cells were seeded onto the untreated, CaP-300 °C and HA/TiO_2-300 °C specimens in a 24-well plate at a density of 2×10^4 cells/well. The amount of cells seeded on the polystyrene (PS) control (2×10^4 cells) was such as to obtain the same cell density used for the coatings.

After one and three days of incubation, the cells adhesion morphology was examined by SEM. The cell proliferation and differentiation were evaluated by methyl thiazole tetrazolium (MTT) and alkaline phosphatase (ALP) assay, respectively.

2.7. MTT assay

MTT assay (reduction of 3-(4, 5-dimethylthiazol-2-yl)-2, 5-diphenyltetrazolium bromide to a purple formazan product) was used to estimate cell viability and proliferation. MTT activity was measured in separate groups of wells (PS, untreated, CaP-300 °C and HA/TiO_2-300 °C specimens). Cells were incubated with 0.5 mg/ml of MTT in the last 4 h of the culture period tested. The media were then decanted, formazan salts were dissolved with 100 μl of dimethyl sulphoxide and absorbance of the solution was measured by a 96-well plate reader (Stat Fax® 2100, Awareness Technology, Inc.) at 540 nm [25].

2.8. Alkaline phosphatase activity

The method of Lowry [26] was used to assay alkaline phosphatase activity in the cell lysates. ALP activity was measured in separate groups of wells (PS, untreated, CaP-300 °C and HA/TiO_2-300 °C specimens). After one, three, seven and 14 days of incubation, medium was removed and the cells were rinsed with PBS, then incubated at 37 °C with 200 μl of substrate solution containing 0.15 M 2-amino-2-methyl-1-propanol buffer, pH = 10.3, 2 mM $MgCl_2$ and 2 mM *p*-nitrophenylphosphate. The reactions were stopped by adding 50 μl of 5 N NaOH to each well and absorbance of the solution was measured by a 96-well plate reader (Stat Fax® 2100, Awareness Technology, Inc.) at 405 nm [27].

2.9. Statistical analysis

Experiments were conducted at least three times and the data shown was one representative experiment. For any given experiment, each data point represented mean ± standard deviation of three individual experiments.

3. Results and discussion

3.1. Crystal structures and surface morphology

The XRD patterns of CaP and HA/TiO_2 coated specimens annealed at various temperature (as-coated, 300 °C, 500 °C and 700 °C), are shown in Figs. 1 and 2. In the CaP as-coated specimen, with deposition current density at 1 mA/cm^2, both dicalcium phosphate dihydrate ($CaHPO_4 \cdot 2H_2O$, DCPD, major) and hydroxyapatite ($Ca_{10}(PO_4)_6(OH)_2$, HA, minor) are found. Their reactions are shown in the following equations [28].

$$Ca^{+2} + HPO_4^{-2} + 2H_2O \rightarrow CaHPO_4 \cdot 2H_2O \quad (1)$$

$$10Ca^{+2} + 6PO_4^{-3} + 2OH^- \rightarrow Ca_{10}(PO_4)_6(OH)_2 \quad (2)$$

The percentage of DCPD in the specimens can be evaluated by the following equation:

$$X(\%) = 100/(1 + 1.265 I_{HA}/I_{DCPD})$$

where I_{DCPD} expresses the intensity of the DCPD peak at $2\theta = 11.65$ (0 2 0) and I_{HA} expresses the intensity of the HA peak at $2\theta = 31.76$ (2 1 1), and X is the weight

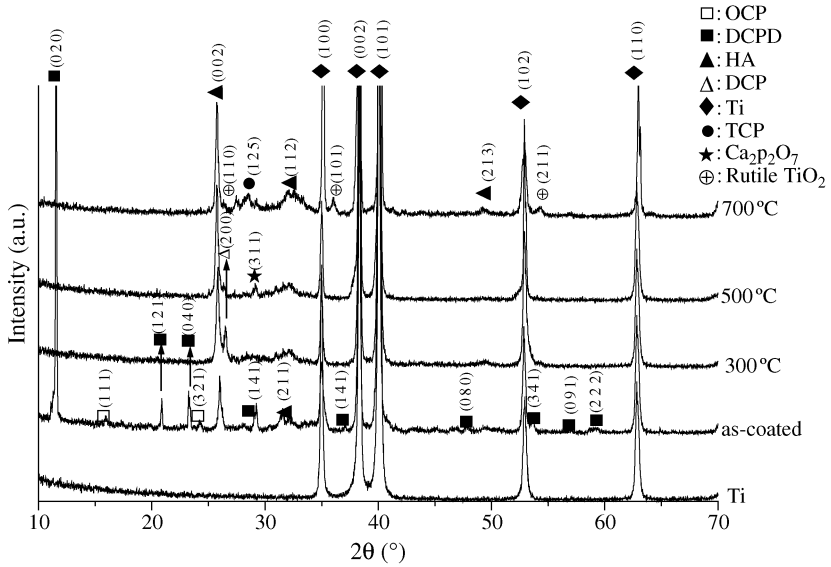

Figure 1 XRD diagrams of CaP coated specimens as-coated and annealed at 300, 500, 700 °C, respectively.

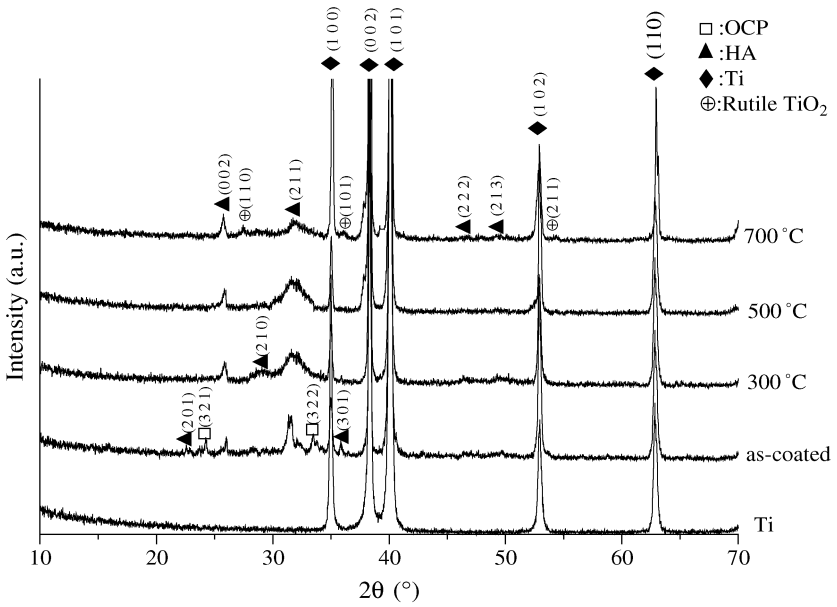

Figure 2 XRD patterns of HA/TiO_2 coated specimens as coated and annealed at 300, 500, and 700 °C, respectively.

percentage of DCPD in the specimen. Therefore, with deposition current density at $1 mA/cm/cm^2$, the CaP as-coated specimen contains 82% DCPD. After annealing at 300 °C, DCPD will phase transformation into dicalcium phosphate ($CaHPO_4$, DCP), but HA still remains. Further annealing at 500 °C DCP will cause phase transformation into calcium pyrophosphate ($Ca_2P_2O_7$). Annealing at 700 °C, HA and $Ca_2P_2O_7$ will result in further phase transformation into tricalcium phosphate ($Ca_3(PO_4)_2$, β-TCP). Therefore, the following reaction is their phase transformation:

$$CaHPO_4 \cdot 2H_2O \xrightarrow{300\,^\circ C} CaHPO_4 + 2H_2O \qquad (3)$$

$$2CaHPO_4 \xrightarrow{500\,^\circ C} Ca_2P_2O_7 + H_2O \qquad (4)$$

$$Ca_{10}(PO_4)_6(OH)_2 + Ca_2P_2O_7 \xrightarrow{700\,^\circ C} 4Ca_3(PO_4)_2 + H_2O \qquad (5)$$

In contrast, HA/TiO_2 as-coated specimens at the same deposition current density of $1 m\mathring{A}/cm^2$ only HA (major) and octacalcium phosphate ($Ca_8(HPO_4)_2(PO_4) \cdot 5H_2O$, OCP, minor) were found. With further annealing at 300 °C, OCP disappeared and only HA was clearly identified on the HA/TiO_2 coated specimens. After annealing above 500 °C, HA/TiO_2 coated samples maintained an HA crystal phase, and did not exhibit phase transformation. Therefore, at the same deposition current density of $1 mA/cm^2$, DCPD did not appear on HA/TiO_2 coated specimens. This was attributed to the high concentration of OH^- supplied by the first deposition of $TiO(OH)_2 \cdot H_2O$ [29]. The very concentrated OH^- environment could transform HPO_4^2 into PO_4^{-3}. Furthermore, in $TiO(OH)_2 \cdot H_2O$ as-coated specimens the cathode polarization curves carried out in a mixed solution of 0.042 M $Ca(NO_3)_2 \cdot 4H_2O$ and 0.025 M $NH_4H_2PO_4$ (pH = 4.76, O_2 = 6.35 mg/l) at 65 °C by an EG&G Princeton Applied Research 273A Potentiostat M352 software also found that OH^- let initial potential (−0.48 V) become more active, compared with titanium substrate (−0.2 V). The result indicated that $TiO(OH)_2 \cdot H_2O$ makes the Ti substrate surface become more alkaline and active to promote the synthesis of HA. Another significant result indicated that HA/TiO_2 coated annealed at 700 °C still remained HA phase, with no phase transformation ($Ca_2P_2O_7$ or β-$Ca_3(PO_4)_2$). In addition, the rutile TiO_2 seen at 700 °C in both CaP and HA/TiO_2 samples as attributed to thermally growth oxide. Pure titanium substrate thermally growth oxide annealed at 300 and 500 °C

TABLE I Corrosion potential E_{corr}, corrosion current density i_{corr}, passivate current density i_{pass}, and polarization resistance R_p of the untreated, TGO-300 °C, EDT-300 °C, EDT-500 °C, EDT-700 °C, CaP-300 °C and HA/TiO_2-300 °C specimens

	E_{corr} (mv)	i_{corr} (nA/cm^2)	i_{pass} ($\mu A/cm^2$)	R_p ($k\Omega$)
Untreated Ti	−406.9	231	2	42.54
TGO-300 °C	−17.19	12.48	0.9	669.4
EDT-300 °C	57.96	1.80	0.05	9519
EDT-500 °C	−46.86	10.32	0.25	1187
EDT-700 °C	−57.72	51.82	0.95	419.6
CaP-300 °C	−182.7	147.9	10	146.8
HA/TiO_2-300 °C	53.45	1.89	0.01	11 460

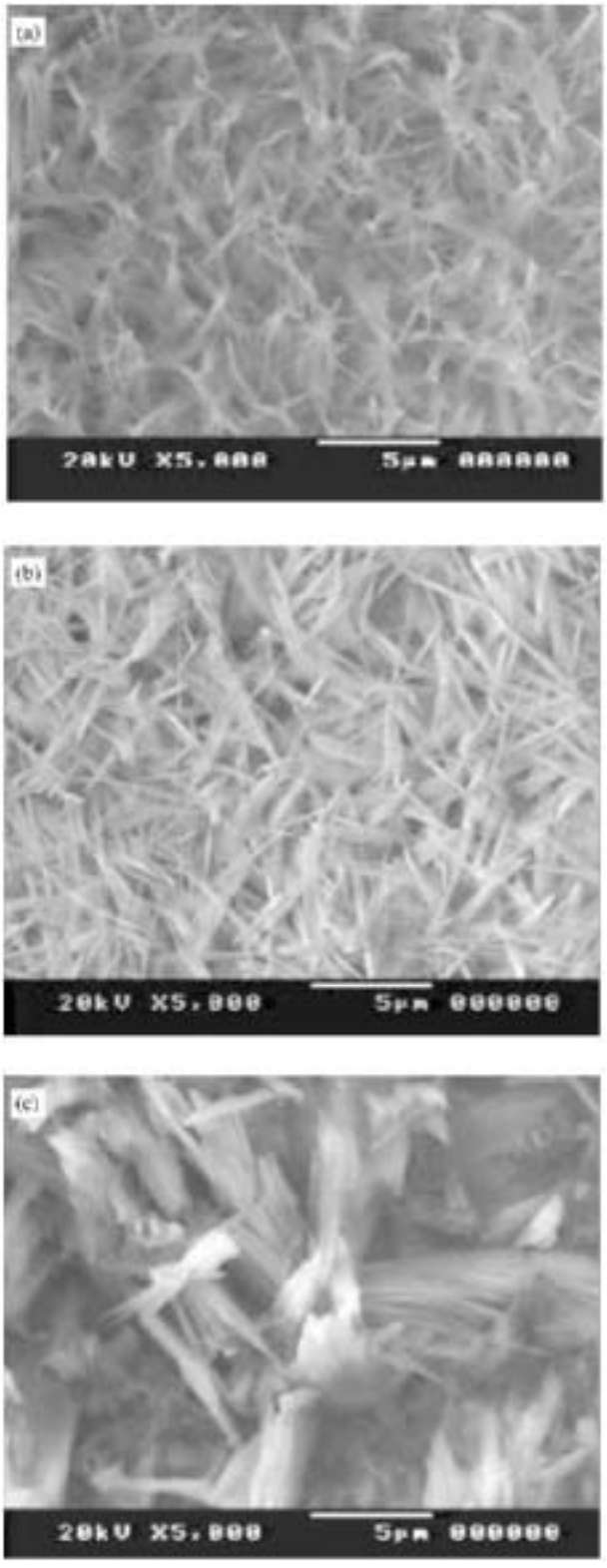

Figure 3 SEM observations of (a) CaP-300 °C, and (b) HA/TiO_2-300 °C specimens upper layer morphology, and (c) HA/TiO_2-300 °C specimen interface layer morphology.

were not appeared TiO_2 crystal phase. However, when annealed temperature up to 700 °C, the rutile TiO_2 was revealed. Further, the rutile TiO_2 is very stable *in vivo*, so it does not cause any effects. Therefore, the HA/TiO_2 coating possessed excellent stability at high temperature.

In SEM images of the surface morphology of CaP-300 °C and HA/TiO_2-300 °C specimens, the upper layer on both appeared needle-like, as shown in Fig. 3(a) and (b). A double layer structure was found on the HA/TiO_2-300 °C specimen. In contrast with the upper layer, the interface layer between the HA and TiO_2 coating showed a feather form and more roughness, as shown in Fig. 3(c).

3.2. Corrosion resistance and immersion tests

The potentiodynamic polarization parameters of the untreated, TGO-300 °C, EDT-300 °C, EDT-500 °C, DET-700 °C, CaP-300 °C and HA/TiO_2-300 °C specimens in SBF solution at 37 °C are given in Table I. It was found that EDT-300 °C specimen has higher corrosion resistance than the TGO-300 °C specimen. Furthermore, we observed that the corrosion potential and protection potential of the HA/TiO_2-300 °C specimen were higher, and the passivation current density and corrosion current density were lower than CaP-300 °C or the untreated. In contrast with the HA/TiO_2-300 °C specimen, the CaP-300 °C specimen expressed poor corrosion resistance as attributed to gaps between the needle-like CaP structures. As the gaps between the needle-like CaP structures present exposed (metal surface) and covered (CaP coated surface) areas, it would induce concentrated cell corrosion. Differential aeration cells would be present, with differing concentrations of dissolved oxygen from exposed and covered areas. In the higher oxygen concentrations areas (exposed titanium substrate), it would fasten to form a protected oxide layer, with the cathode reduction reaction of $O_2 + 2H_2O + 4e^- \rightarrow 4OH^-$. On the other hand, lower oxygen concentrations areas (covered with CaP coated surface) would be limited in forming a protected oxide layer and thus further induce corrosion. The cathode reduction reaction was $2H_2O + 2e^- \rightarrow 2OH^- + H_2$. Apparently, the HA/$TiO_2$-300 °C specimen exhibited the greatest corrosion resistance by adding the dense intermediate TiO_2 coating. The higher E_{corr}, lower i_{corr}, lower i_{pass} and higher polarization resistance R_p of the HA/TiO_2-300 °C coated specimens indicated that the coated film was more resistant to corrosion or more inert than the natural passive film of pure Ti and a CaP-300 °C specimen.

For immersion tests, weight variation was observed on untreated, CaP-300 °C and HA/TiO_2-300 °C specimens

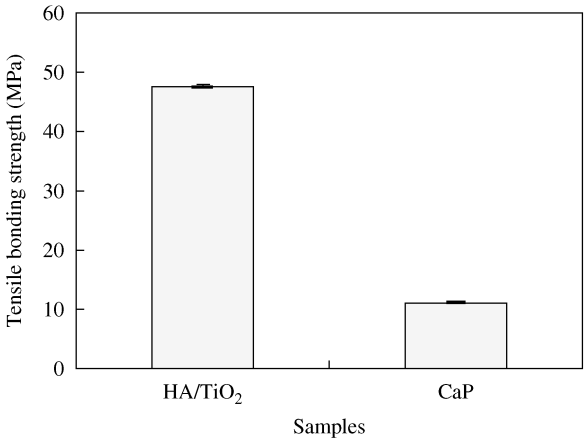

Figure 4 Bonding strength of CaP-300 °C and HA/TiO_2-300 °C coating proceed tensile tests.

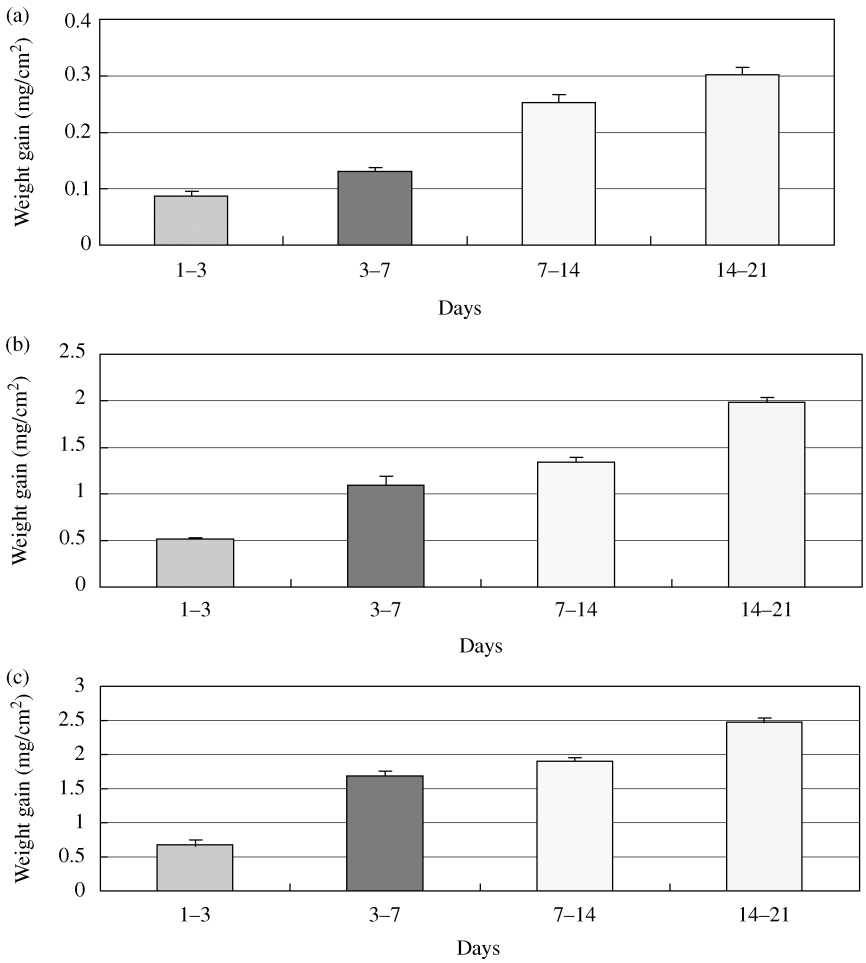

Figure 5 Plots of weight gain vs. immersion time for (a) untreated, (b) CaP-300 °C and (c) HA/TiO_2-300 °C specimens in SBF solution at 37 °C.

in SBF solution, as shown in Fig. 5. However, the weight gains of the CaP-300 °C and HA/TiO_2-300 °C specimens were more than that of the untreated specimen. The XRD diagrams of the HA/TiO_2-300 °C specimen after immersion tests indicated that the crystallization was increased with increasing time. The HA (2 1 1) preferred orientation intensity was increasing with immersion time, as shown in Fig. 6. Obviously, the apatite further precipitates and grows on HA/TiO_2 coatings in a preferred orientation. After three days, we observed that apatite precipitated along the dendrities to form a column structure. After seven days, apatite precipitate completely covered the HA/TiO_2 coated surface, as shown in Fig. 7. The results indicated that electrolytic

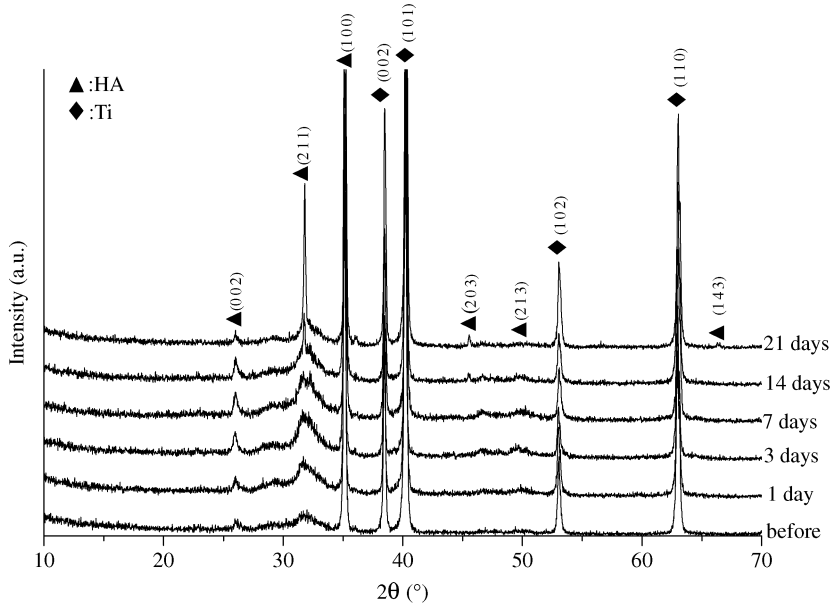

Figure 6 XRD patterns of HA/TiO_2-300 °C specimens immersed in SBF solution for one, three, seven, 14, and 21 days, respectively.

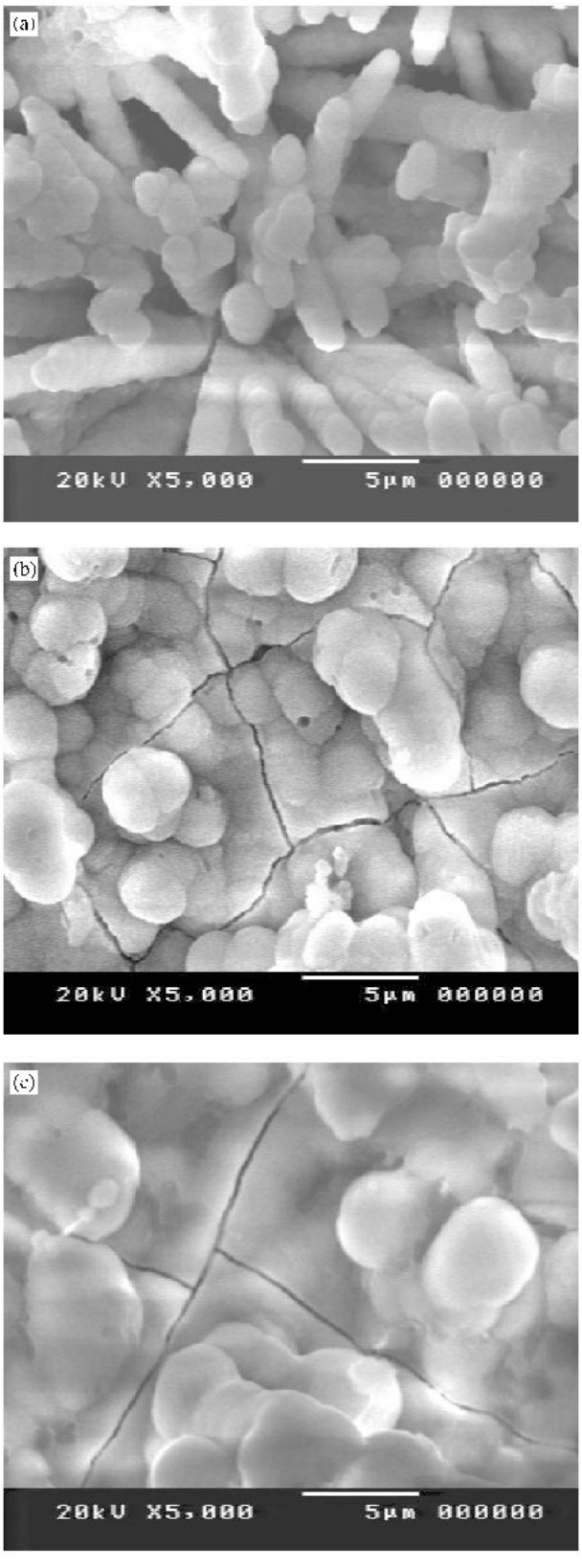

Figure 7 SEM observation of HA/TiO_2-300 °C specimen immersed in SBF solution for (a) three days, (b) seven days, and (c) 14 days.

deposition of a HA/TiO_2 coating expressed more bioactivity than the untreated titanium substrate in the SBF solution.

3.3. Tensile tests and cross-section observations

The CaP-300 °C and HA/TiO_2-300 °C specimens underwent tensile tests. In contrast with CaP coated samples, the HA bonding strength improved from 11.3 to 46.7 MPa by adding the intermediate electrolytic deposition of TiO_2, as shown in Fig. 4. The significance of this result is the indication that $TiO(OH)_2 \cdot H_2O$ gel not only promoted the HA synthesis, but after annealing at 300 °C it would provide a chemical bonding to increase bonding strength. The excellent adhesion was attributed to the condensation of $TiO(OH)_2 \cdot H_2O$ with OH^- bonds adsorbed on Ti substrate and OH^- bonds of HA to form the very strong Ti–TiO_2–HA chemical bonding. Such a condensation would happen at $T \geq 300$ °C. TiO_2 intermediate coating improved the bonding strength of the subsequently HA-coated samples.

The SEM cross-section observations of EDT-300 °C, CaP-300 °C and HA/TiO_2-300 °C specimens are shown in Fig. 8. The thickness of EDT-300 °C, CaP-300 °C and HA/TiO_2-300 °C specimens were about 1.2, 10 and 12 µm, respectively. In HA/TiO_2-300 °C specimens, the EDS profiles of the elements Ti, P and Ca revealed that some HA had been mixed into the TiO_2 layer, as shown in Fig. 8(c). The intermixing of TiO_2 and HA also acted as another factor, which resulted in the extremely high-adhesion strength. The composition of this coating presented a concentration gradient (from a TiO_2 at the substrate surface through a composite coating to a HA at the implant/body interface). The objective is to add a TiO_2–TiO_2 chemical component to the binding between the titanium substrate (spontaneous TiO_2) and the coating (electrolytic TiO_2) to increase the adhesion strength.

3.4. Cell proliferation and differentiation assay

Untreated, CaP-300 °C and HA/TiO_2-300 °C specimens were assessed by cell activity assay. Using a 24-well culture plate, cells grown on the biomaterials-coated polystyrene (PS) well were used as the control. According to the results of MTT assay, after one day the mirror polished Ti surface and needle-like CaP-300 °C sample exhibited higher proliferation, as shown in Fig. 9(a). After three days, clear contrast occurred on the CaP-300 °C specimen. This serious decrease of cell proliferation was attributed to dissolvtion of DCP, because DCP dissolution would contribute to osteoinductive properties. In contrast, mirror-polished Ti surface still appeared to show higher proliferation, as shown in Fig. 9(b). After seven and 14 days, cell proliferation on mirror-polished Ti surface obviously decreased, and on needle-like CaP-300 °C and HA/TiO_2-300 °C specimens gave evident increase, as shown in Fig. 9(c) and (d). In the other test results, Fig. 10 shows the cell differentiation on various samples. There are no detectable amounts of alkaline phosphatase activity by cell culture on all substrates tested in the present study after seven days of culture. It could be observed that until 14 days cell differentiation on the CaP-300 °C and HA/TiO_2-300 °C needle-like coated specimens had evident increase, in contrast with PS and mirror-polished Ti substrates. The relationship can be established between the surface morphology and the cell growth: on mirror polished Ti surface, the lower frequency of adhering pseudopodia is correlated to an increase of cell proliferation. Indeed, cell growth better

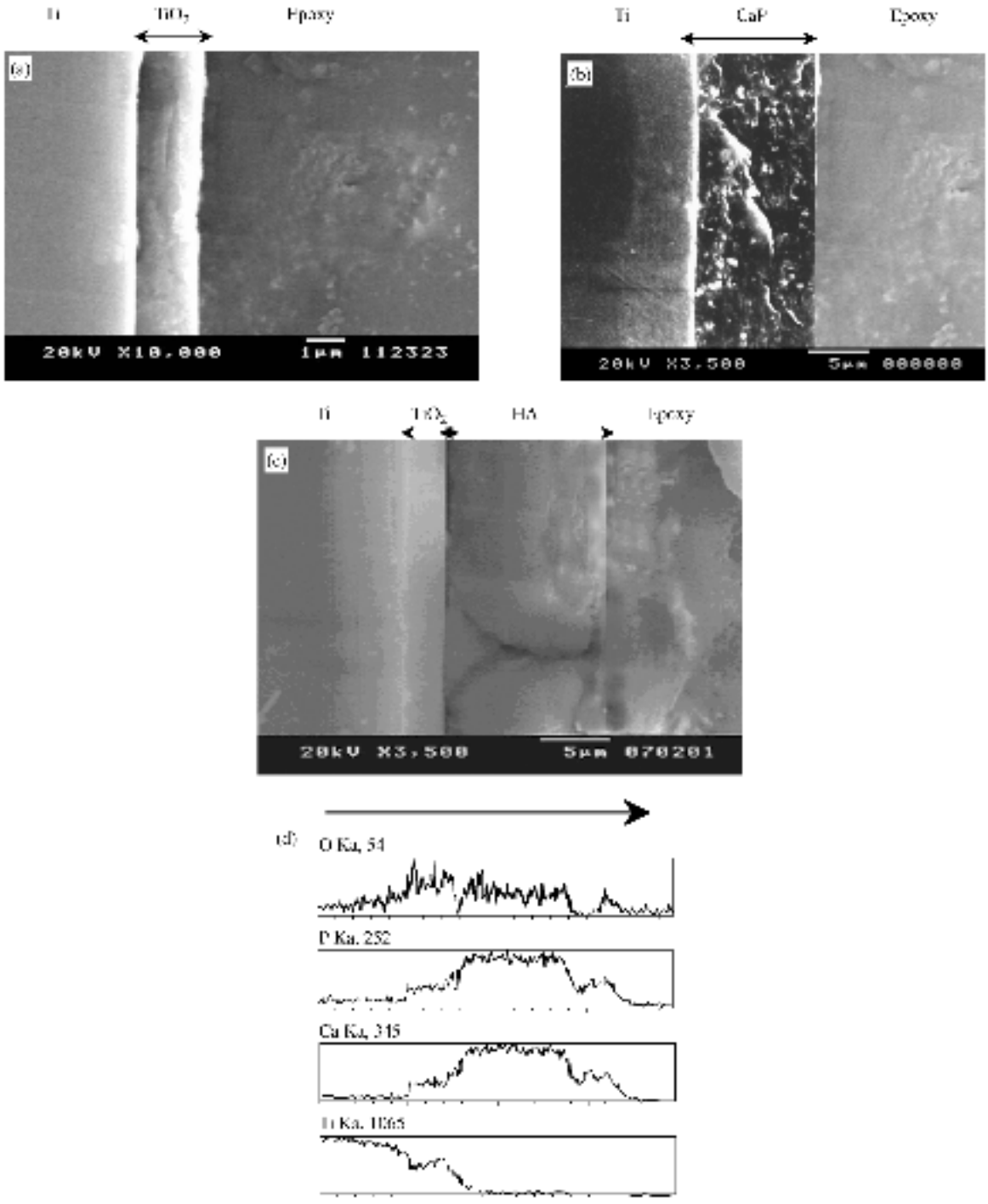

Figure 8 SEM cross-section observations (a) EDT-300 °C, (b) CaP-300 °C, (c) HA/TiO_2-300 °C specimens and (d) EDS line profiles of O, P, Ca, Ti on HA/TiO_2-300 °C specimen.

occurs when cell adhesion is decreased. This has been demonstrated for cell/substrate (biomaterials) and cell/cell interaction [30].

On the other hand, the rapid cell proliferation and the lower cell differentiation of mirror polished Ti surface may lead to a retarded hard tissue formation and subsequently to a delayed implant load. In contrast, needle-like HA/TiO_2-300 °C specimens seems to be a convenient compromise on the cell proliferation and cell differentiation.

4. Summary and conclusions

A novel electrolytic coating method of HA/TiO_2 double layers has been successfully conducted on pure titanium to investigate its characteristics. Through the electrolytic deposition, annealing, dynamic cyclic polarization tests, immersion tests, surface observations, XRD analysis, tensile tests and cell culture assays, several conclusions are drawn

1. The previous TiO_2 coating and/or the further annealing had the effect of reducing the amount of DCPD and OCP in HA, and the crystallization of HA on the CaP and HA/TiO_2 coated specimens annealed at 300 °C was the best. In addition, TiO_2 coating also stabilized the HA-coated film to avoid high temperature phase transformation ($Ca_2P_2O_7$ and β-$Ca_3(PO_4)_2$).

2. The adhesion strength of electrolytic deposited HA on a Ti substrate was dramatically improved from

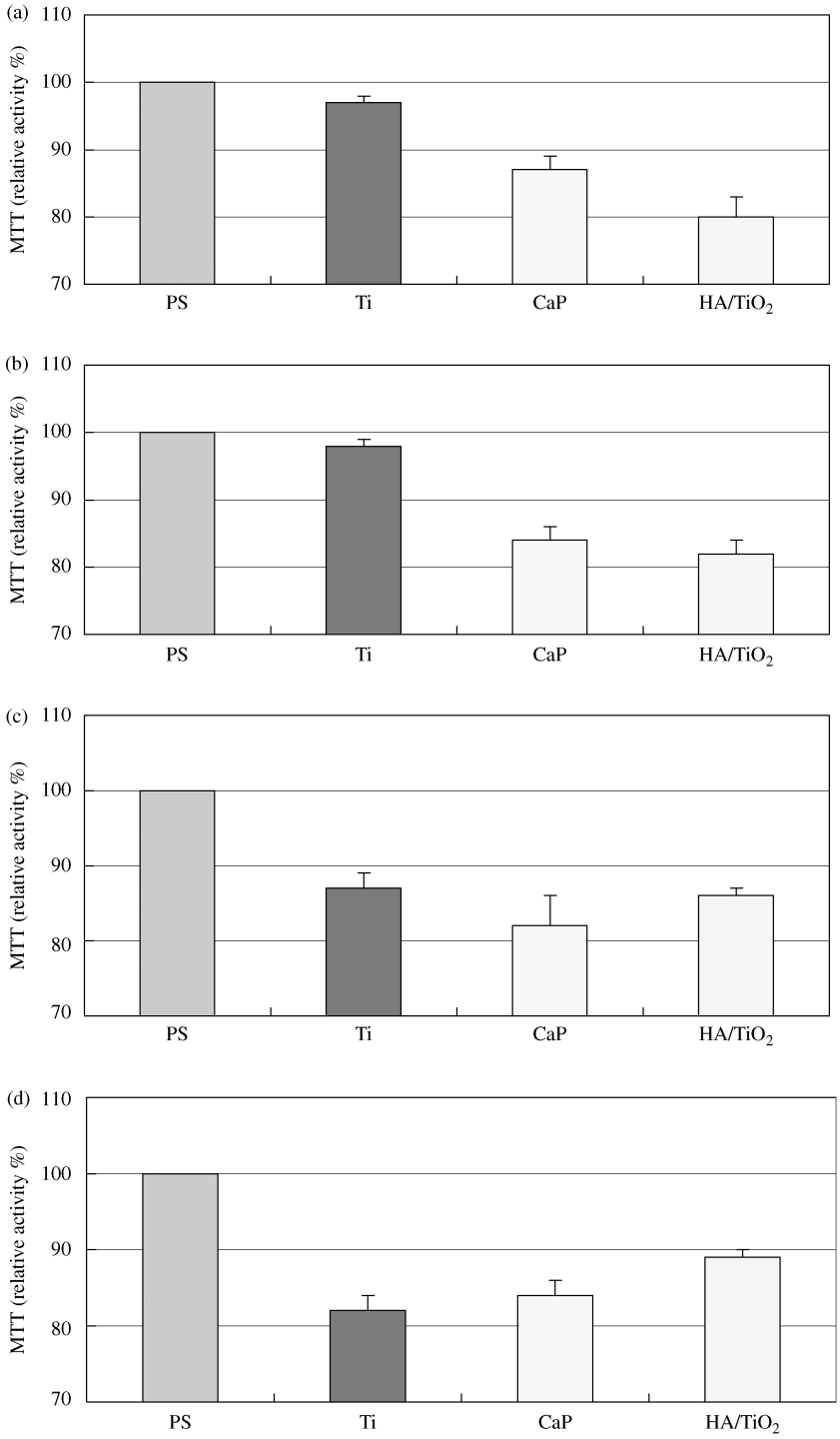

Figure 9 MTT assay showing relative activity of the G-292 osteoblast-like cells after (a) one day, (b) three days, (c) seven days and (d) 14 days grown on PS, untreated Ti, CaP-300 °C, and HA/TiO_2-300 °C specimens.

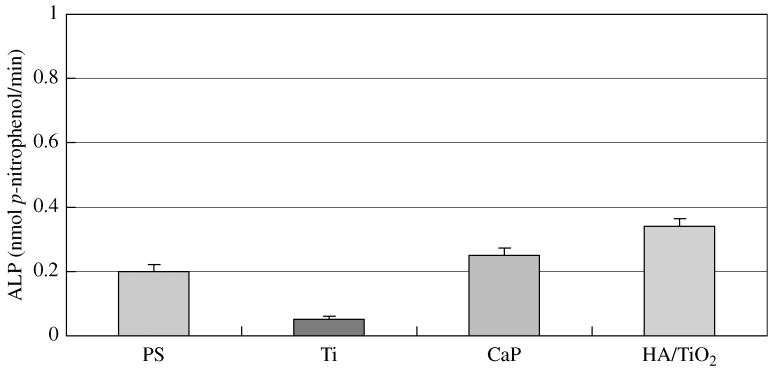

Figure 10 Alkaline phosphatase activity of the G-292 osteoblast-like cells after 14 days grown on PS, untreated Ti, CaP-300 °C, and HA/TiO_2-300 °C specimens.

11.3 to 46.7 MPa by adding the intermediate electrolytic deposition of TiO_2, which showed the strong chemical bonding effects between the Ti alloy substrate and HA coating.

3. The polarization tests in SBF solution revealed that the HA/TiO_2-300 °C coating was the most corrosion resistance. Both CaP-300 °C and HA/TiO_2-300 °C specimens exhibited (2 1 1) preferred-orientation with respect to HA itself. After immersion tests in SBF solution, the apatite further precipitated and grew on HA/TiO_2 coatings in preferred orientation. The results indicated that electrolytic deposition of HA/TiO_2 double layers expressed more bioactivity than the titanium substrate in the SBF solution.

4 The cell activity assay indicated that the electrolytic deposition HA/TiO_2 coatings on pure titanium substrates were nontoxic to the cells. Furthermore, the materials characteristics such as surface morphology, corrosion resistance, and phase component may play an important role in the osteointegration.

Acknowledgments

The authors are grateful for the support of this research by the National Sciences Council, Republic of China, under contract No. NSC 91-2213-E-005-014.

References

1. F. WATARI, A. YOKOYAMA, F. SASO, M. UO and T. KAWASAKI, *Composites Part B: Eng.* **28B** (1997) 5.
2. P. L. BATAILLON, F. MONCHAU, M. BIGERELLE and H. F. HILDEBRAND, *Biomol. Eng.* **19** (2002) 133.
3. C. H. KU, D. P. PIOLETTI, M. BROWNE and P. J. GREGSON, *Biomaterials* **23** (2002) 1447.
4. I. DEGASNE, M. F. BASLE, V. DEMAIS, G. HURE, M. LESOURD, B. GROLLEAU, L. MERCIER and D. CHAPPARD, *Calcif. Tissue Int.* **64** (1999) 499.
5. X. NIE, A. LEYLAND and A. MATTHEWS, *Surf. Coat. Technol.* **125** (2000) 407.
6. H. KURZWEG, R. B. HEIMANN, T. TROCZYNSKI and M. L. WAYMAC, *Biomaterials* **19** (1998) 1507.
7. D. J. LI, K. OHSAKI, K. LI, P. C. CUI, O. YE, K. BABA, Q. C. WANG, S. TENSIN and T. Y. TERUKO, *J. Biomed. Mater. Res.* **45** (1999) 322.
8. A. M. EKTESSABI and H. KIMURA, *Thin Solid Films* **270** (1995) 335.
9. G. K. DE, R. GEESINK, CPAT. KLEIN and P. SEREKIAN, *J. Biomed. Mater. Res.* **121** (1987) 1357.
10. R. MCPHERSON and N. GANE, *J. Mater. Sci.: Mater. Med.* **6** (1995) 327.
11. H. KURZWEG and R. B. HEIMANN, *Biomaterials* **19** (1998) 1507.
12. K. V. DIJK, H. G. SCHAEKEN, J. G. G. WOLKE and J. A. JANSEN, *ibid.* **17** (1998) 159.
13. O. YOSHINO and M. MASAMICHI, *Surf. Coat. Technol.* **65** (1994) 224.
14. C. K. WANG and L. J. H. CHERN, *Biomaterials* **18** (1997) 1331.
15. R. DAMODARAN and B. M. MOUDGIL, *Colloids Surface A: Physicochem. Eng. Aspects* **80** (1993) 191.
16. W. WENG and J. L. BAPTISTA, *J. Am. Ceram. Soc.* **82** (1999) 27.
17. W. WENG and J. L. BAPTISTA, *J. Mater. Sci.: Mater. Med.* **9** (1998) 159.
18. H. HERO, H. WIE and R. B. JORGENSEN, *J. Biomed. Mater. Res.* **28** (1994) 343.
19. P. G. BRADFORD, J. M. MAGLISH, A. S. PONTICELLI and K. L. KIRKWOOD, *Arch. Oral Biol.* **45** (2000) 159.
20. Designation: C-633. Standard test method for adhesion of cohesive strength of flame-sprayed coatings, Annual Book of ASTM Standards, American Society for testing and materials, Philadelphia, PA, vol. 3.01, 1993, p. 665.
21. H. M. KIM, F. MIYAJI, T. KOKUBO and T. NAKAMURA, *J. Biomed. Mater. Res.* **38** (1997) 121.
22. T. KOKUBO, H. M. KIM and M. KAWASHITA, *Biomaterials* **24** (2003) 2161.
23. S. K. YEN and C. M. LIN, *J. Electrochem. Soc.* **149** (2002) 79.
24. K. L. KIRKWOOD, R. DZIAK and P. G. BRADFORD, *J. Bone Mineral. Res.* **11** (1996) 1889.
25. P. A. RAMIRES, A. ROMITO, F. COSENTINO and E. MILELLA, *Biomaterials* **22** (2001) 1467.
26. O. H. LOWRY, N. R. ROBERTS, M. L. WU, W. S. HIXON and E. J. CRAWFORD, *J. Biomed. Chem.* **207** (1954) 19.
27. R. J. MAJESKA, J. T. RYABY and T. A. EINHORN, *J. Orth. Res.* **20** (2002) 281.
28. S. K. YEN and C. M. LIN, *Mater. Chem. Phys.* **77** (2002) 70.
29. C. M. LIN and S. K. YEN, in Proceedings of the 8th Biomedical Materials and Technology Symposium, Taiwan, ROC September (2003) A101.
30. A. BEN-ZE'EV, *Curr. Opin. Cell Biol.* **9** (1997) 99.

Received 20 October 2003
and accepted 27 April 2004